Effects of Surface Treatments on Mechanical Behavior of Sintered and Pre-sintered Yttria-Stabilized Zirconia and Reliability of Crowns and Abutments Processed by CAD/CAM

Talita Souza Dantas, PhD, MSc, DDS[1]/Renata Cristina Silveira Rodrigues, PhD, MSc, DDS[1]/
Lucas Zago Naves, PhD, MSc, DDS[2]/Adriana Cláudia Lapria Faria, PhD, MSc, DDS[1]/
Regina Guenka Palma-Dibb, PhD, MSc, DDS[3]/Ricardo Faria Ribeiro, PhD, MSc, DDS[1]

Purpose: This study evaluated the micro shear bond strength of resin cement to an yttria-stabilized zirconia ceramic and the survival probability of zirconia abutments and crowns after different surface treatments through a fatigue test. **Materials and Methods:** The study was divided into two parts. For part 1, 95 zirconia disks were divided into five groups (n = 19): control, untreated, airborne particle abrasion with Al_2O_3 particles before sintering, airborne particle abrasion with Al_2O_3 particles after sintering, silicatization before sintering, and silicatization after sintering. Three samples of each group were used for evaluation of surface roughness by confocal laser scanning microscopy and afterward were prepared for surface microstructural analysis by scanning electron microscopy. Ten samples of each group were subjected to micro shear bond strength testing, and the interfaces of the remaining six were examined by scanning electron microscopy. In part 2, 70 external hex zirconia abutments and copings were made by computer-aided design/computer-aided manufacturing (n = 14). Marginal fit of abutment/coping was measured in a confocal laser scanning microscope. Afterward, a fatigue test was carried out with progressive load of 80 up to 320 N (40 N steps), 5 Hz frequency, and 20,000 cycles at each step. Thermal cycling was simultaneously performed (5°C to 55°C). **Results:** The group treated after sintering with SiO achieved statistically higher micro shear bond strength (P < .01). Higher failure loads were associated with a combined failure. The surface changes in the group treated with SiO before sintering suggest silica deposition, and there was a lack of homogeneity, which was more evident on the surface of the groups treated before sintering. The marginal gap was higher for the group treated before sintering with SiO (P < .01), and the survival probability of the sets was similar for all tested groups (P = .57). **Conclusion:** The micro shear bond strength to zirconia was improved after silicatization after sintering, but the survival probability of crown/abutment/implant sets was not affected by different surface treatments. INT J ORAL MAXILLOFAC IMPLANTS 2019;34:907–919. doi: 10.11607/jomi.7294

Keywords: marginal gap, surface treatment, thermomechanical fatigue, zirconia

[1]Department of Dental Materials and Prosthodontics, School of Dentistry of Ribeirao Preto, University of São Paulo (USP), Ribeirao Preto, Brazil.

[2]Department of Direct Restorative and Biomaterials, Center for Dentistry and Oral Hygiene, University Medical Center Groningen, The University of Groningen, Groningen, The Netherlands.

[3]Department of Restorative Dentistry, School of Dentistry of Ribeirao Preto, University of Sao Paulo (USP), Ribeirao Preto, Brazil.

Correspondence to: Dr Ricardo Faria Ribeiro, Department of Dental Materials and Prosthodontics, School of Dentistry of Ribeirao Preto, University of São Paulo – USP, Av. do Café, SN, Monte Alegre, 14040-904, Ribeirao Preto, SP, Brazil. Email: rribeiro@forp.usp.br

Zirconia has increasingly been used in oral rehabilitation because computer-aided design/computer-aided manufacturing (CAD/CAM) technology simplified the fabrication of crowns or prosthesis frameworks with this material of high crystalline content.[1] Although it has good esthetic, biologic, and mechanical properties, adhesion to zirconia is still a challenge.[2]

Before cementation, surface treatment with hydrofluoric acid etching and silanization is necessary for satisfactory adhesion to ceramics, but the same treatment is not enough for resin bond to zirconia because they lack a silica phase.[3,4]

Therefore, several surface treatments have been proposed to improve bonding to zirconia ceramics. Airborne particle abrasion is an option for surface treatment because an acceptable roughness is created,

Table 1 Groups and Parameters Used for Surface Treatments

Group	Treatment[a]	Moment	Distance/time (mm/s)	Pressure (bar)
C	–	–	–	–
ALS	110 µm Al_2O_3	After sintering	20/15	3
ROS	110 µm SiO[b]	After sintering	20/15	3
AL	110 µm Al_2O_3	Before sintering	25/8	1.5
RO	110 µm SiO[b]	Before sintering	25/8	1.5

[a]Airborne particle abrasion; [b]Rocatec Plus (3M ESPE).
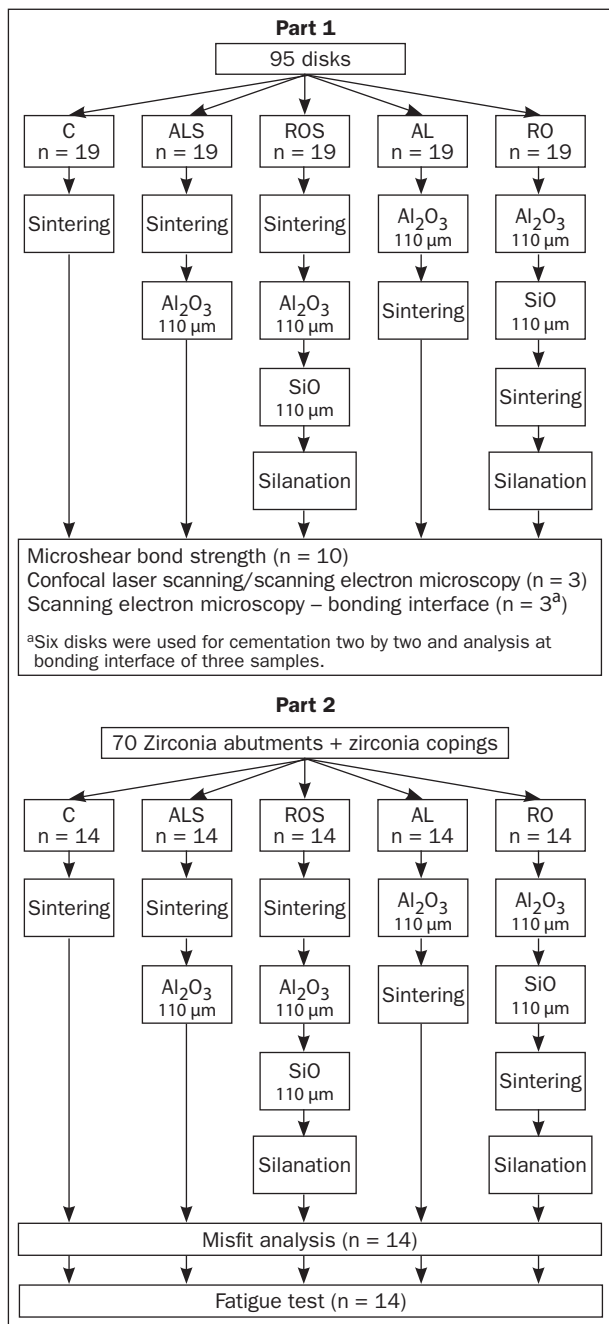
Fig 1 Study workflow.

increasing surface area and allowing resin/ceramic micromechanical interlock formation.[5,6] Another surface treatment proposed for zirconia frameworks is chairside air abrasion with 30-µm or 100-µm silica-coated aluminum particles (tribochemical silica coating, also known as silicatization), leading to silica being embedded onto the ceramic surface.[7,8] Bonding to resins is enhanced in these surfaces because silane coupling agents react with silica-coated aluminum particles,[8] but changes caused by these surface treatments in ceramic topography are still unclear.

A recent study has suggested that airborne particle abrasion with Al_2O_3 should not be used, particularly with yttria-stabilized zirconia, because it could result in micro fractures that can reduce their functional strength, which can lead to premature and catastrophic failures.[9] However, airborne-particle abrasion of yttria-stabilized zirconia surfaces before sintering could improve the resin bond strength to this ceramic without damaging the microstructure. Still, little is known regarding the surface modification of these ceramics prior to the sintering process,[10] and the effects of these surface treatments on the mechanical behavior of crowns and abutments are unknown.

The aim of the present study was to evaluate the micro shear bond strength of a resin-based cement to an yttria-stabilized zirconia submitted to different surface treatments, and afterward to assess the survival probability and failure mode of zirconia crowns bonded to zirconia abutments obtained from a CAD/CAM system, all after different surface treatments, through an in vitro fatigue test. Additionally, misfit measurements were assessed. The null hypothesis was that the surface treatments would not influence the micro shear bond strength of zirconia to resin cement, the survival probability, and failure mode of the zirconia crowns bonded to zirconia abutments.

MATERIALS AND METHODS

The present study evaluated the effect of different surface treatments of zirconia for cementation through evaluation of micro shear bond strength of a resin-based cement to zirconia, and evaluation of in vitro fatigue resistance and failure mode of zirconia crowns bonded to zirconia abutments.

Surface Treatments

The groups were divided according to the surface treatment proposed (Table 1), and the study followed the workflow presented in Fig 1.

According to the manufacturer recommendations, the groups to be treated with SiO previously received airborne particle abrasion with 110 µm Al_2O_3 to clean

and activate the surface, and after airborne particle abrasion with SiO, a silane coupling agent (RelyX Ceramic Primer, 3M ESPE) was applied to obtain chemical bonding.

Part 1: Micro Shear Bond Strength of a Resin-Based Cement to Zirconia

Specimen Description and Manufacture. Ninety-five disk-shaped yttria-stabilized zirconia specimens (NEOSHAPE, Neodent) (Ø = 12.6 × 2.0 mm thickness) were produced by CAD/CAM following the manufacturer recommendations. All specimens were cleaned with deionized water in ultrasonic bath for 10 minutes (Ultrasonic Cleaner 144OD, Odontobrás), and randomly allocated into groups (n = 19).

For surface treatment, airborne particle abrasion was performed in a dynamic way, with constant movements along a 180-degree axis for the time determined in each group to obtain an entire surface that was treated and not only a point (Fig 2).

Micro Shear Bond Strength Test. After treatments, disks (n = 10) were prepared for the micro shear bond strength test, embedded in polyurethane (F-16 Fastcast Polyurethane, Axson) with the treated surface exposed. In each disk, three cylinders (1.2-mm diameter; 1.2-mm height) of resin cement (RelyX U200, 3M ESPE) were produced using a template. The resin cement was applied using an explorer probe in the template orifices and light cured for 40 seconds. The template was removed, and the specimens were analyzed in a stereomicroscope (S8APO, Leica Microsystems) with a digital camera (DFC295, Leica Microsystems) to certify that there were no bubbles or defects in the cylinders. All specimens were then stored in 100% humidity at 37°C for 24 hours prior to micro shear bond strength testing.[11]

For micro shear bond strength testing, every disk specimen was attached in an adapted device fixed to a universal testing machine (DL 2000, EMIC) with a thin stainless steel wire (0.2-mm diameter) placed around each cylinder, as close as possible to the bonding interface. The test was performed at a speed of 1 mm/minute with a load cell of 5 kg until failure occurred, and the micro shear bond strength data were recorded in Megapascals (MPa). For each group evaluated, 30 cylinders were tested, three per ceramic disk (n = 10).

Failure Mode Analysis. After the micro shear bond strength test, all specimens were analyzed under stereomicroscopy (S8APO, Leica Microsystems) with a digital camera (DFC295, Leica Microsystems) to assign the predominant failure mode: adhesive failure, no cement remaining on the disk surface; cohesive failure, cement remaining on the disk with cement failure; and mixed failure, a mix of cohesive and adhesive failures. The results of the failure classification within each substrate were subjected to percentile distribution.

Fig 2 Adjustable device. *(a)* Jet tip is fixed. *(b)* Disk is positioned and can rotate 180 degrees.

Scanning Electron Microscopy Evaluation of Bonding Interfaces. To observe the morphology at the bonding interfaces, six additional disks were obtained for each group and cemented two by two (n = 3),[12] according to manufacturer recommendations, under a cement load of 5 kg for 10 minutes. The specimens were completely embedded in polyurethane and longitudinally cross-sectioned (IsoMet, Buehler) to expose the disk-cement-disk interface. The specimens were then wet-polished with 600-, 1,200-, and 2,000-grit SiC paper. The cross-section profiles were examined by scanning electron microscopy (Phenom G2 PRO, Phenom World BV), focusing on the depth of the cement penetration; micromechanical entanglement; and the integrity, homogeneity, and continuity along the bonding interface.

Scanning Electron Microscopy and Confocal Laser Scanning Microscopy Evaluation of Surface Morphology. In addition, three specimens of each group (n = 3) were used to observe the surface morphology by confocal laser and scanning electron microscopy. A three-dimensional (3D) confocal laser scanning microscopy analysis (LEXT 3D Measuring Laser Microscope OLS4000, Olympus) was performed, focusing on the surface modifications and roughness after each treatment. Objective lens of 100× and 2,132× magnification were used. Ten images were obtained from each of the three additional specimens before scanning electron microscopy evaluation, with a representative image chosen based on similarities and repetitive patterns. Fields of view at a 130 × 130-μm scan size were considered to analyze the average surface roughness (Ra) of the zirconia after the different surface treatments, expressed as a numeric value (μm). Five measurements were performed for each pretreated ceramic disk. After 3D confocal laser scanning microscopy analysis, the same samples were evaluated by scanning electron microscopy.

Statistical Analysis

For micro shear bond strength results, a specific software package (SAS 9.0, SAS Institute) was used for the statistical analysis. In this case, the mixed effect linear regression model did not show normal distribution, so a logarithmic transformation was necessary. Also, the Tukey test was used at a confidence interval of 95% and a significance level of $P < .01$.

Part 2: Fatigue Resistance and Failure Mode of Zirconia Crowns Bonded to Zirconia Abutments

Specimen Description and Manufacture. Seventy external hex implant analogs ($\varnothing$ = 4.1 mm) (Neodent) were included in polyurethane resin (F-16 Fastcast Polyurethane, Axson), with inclination of 30 degrees according to norm ISO 14801. Associated with the analogs, 70 zirconia abutments and 70 zirconia copings were obtained by CAD/CAM (NEOSHAPE, Neodent) and allocated into groups (n = 14).

The inner surfaces of copings of the RO and AL groups were treated before sintering, while those of the ROS and ALS groups were treated after sintering as described earlier.

Misfit Analysis and Veneer Manufacture. Fits of copings on the abutments were measured in four preset points (vestibular, mesial, distal, and palatal) of marginal perimeter between the surface of the abutments and copings for the five groups (n = 14) with confocal laser scanning microscopy (LEXT 3D Measuring Laser Microscope OLS4000, Olympus). An abutment of each group was fixed on an implant analog, and copings were juxtaposed with a shield, allowing a 90-degree visualization with the microscope. Fields of view of 1,281 $\times$ 1,281 µm (scan size) were considered to obtain the images and subsequent measurement of marginal gap in micrometers (µm). Three measurements in each of the four predetermined points were made, and the average was obtained.

After coping marginal misfit analysis, they were veneered with the IPS e.max ZirPress ceramic system (Ivoclar Vivadent). A representative canine wax sculpture (Rainbow) was made, and a silicone matrix (Flexitime, Heraeus Kulzer) enabled the duplication in wax sculpture over existing copings.

Abutment Placement and Crown Luting. The inner surfaces of copings from groups treated with SiO, before and after sintering, were primed with RelyX Silane agent (3M ESPE) to establish a chemical bond with the resin cement, following the manufacturer's recommendations. Before cementation, a 32-Ncm torque was applied to Neotorque screws (Neodent), and the holes were sealed with Teflon tape. The crowns were luted to the abutment using resin cement (RelyX U200, 3M ESPE), and the material was inserted inside each crown and manually positioned on the abutment. A device with 439 g was used to seat the crowns on the abutments using a dental surveyor. After removal of the resin cement excesses with hand instruments (scaler, blade), all surfaces were light polymerized for 20 seconds each, and then, specimens were stored in distilled water for 24 hours before testing.[11]

Fatigue Test. The analog-abutment-crown sets (n = 14) were subjected to a cyclic mechanical test (Biopdi). The chewing cycle was simulated by an isometric contraction (load control) applied through a flat antagonist (made of composite resin Z100; 3M ESPE) according to norm ISO 14801. Cyclic load was applied at a frequency of 5 Hz, starting at 80-N load, followed by stages of 120, 160, 200, 240, 280, and 320 N, with a maximum of 20,000 cycles each. Samples were loaded until fracture or to a maximum of 140,000 cycles.[13,14] Simultaneously with the mechanical cycling, the samples were subjected to thermal cycling with temperatures ranging between 5°C and 55°C and immersion time of 40 seconds. The number of endured cycles and failure mode were recorded. The failure modes were classified as: abutment failure (type I), veneer failure (type II), coping failure (type III), abutment and coping failure (type IV), or abutment and veneer failure (type V).
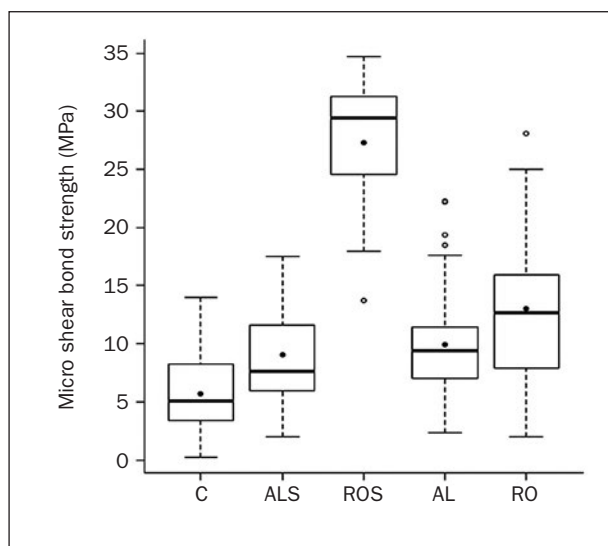
Statistical Analysis

The fatigue resistance of all groups was compared using the life table survival analysis. At each time interval (defined by each load step), the number of specimens starting the interval intact and the number of specimens fracturing during the interval were counted, allowing the calculation of survival probability at each interval. The survival probability was determined as a percentage, and the closer to 100%, the greater the chance of no failure in certain load. The log-rank test at a significance level of .05 was used to compare the groups. The Spearman correlation coefficient was used to verify the correlation between misfit values and number of cycles and load stage.

RESULTS

Part 1: Micro Shear Bond Strength of a Resin-Based Cement to Zirconia

Micro Shear Bond Strength Test. The results of failure load (MPa) for the micro shear bond strength test are presented in Fig 3. The linear regression model with mixed effects and Tukey's test showed that specimens treated with SiO after sintering achieved statistically higher ($P < .01$) micro shear bond strengths compared with all other surface treatments, suggesting a strong interaction between silica coating and the silane after

Fig 3 Micro shear bond strength results.

Table 2 Micro Shear Bond Strength (MPa) Comparison Among Different Surface Treatments

Comparison	Mean difference	P value	Confidence interval Lower limit	Confidence interval Upper limit
AL × ALS	0.85	.99	−4.53	6.22
AL × C	4.21	.20	−1.20	9.62
AL × RO	−2.76	.62	−8.19	2.66
AL × ROS	−17.56	< .01	−22.96	−12.17
ALS × C	3.37	.42	−2.03	8.76
ALS × RO	−3.61	.35	−9.02	1.80
ALS × ROS	−18.41	< .01	−23.79	−13.03
C × RO	−6.98	< .01	−12.42	−1.54
C × ROS	−21.78	< .01	−27.19	−16.37
RO × ROS	−14.80	< .01	−20.23	−9.37

sintering. There was no significant difference between untreated (control) and treated with Al_2O_3 after sintering ($P = .42$) and between untreated (control) and treated with Al_2O_3 before sintering ($P = .20$) (Table 2).

Failure Mode Analysis. Untreated specimens demonstrated only adhesive failures. All surface treatments, after and before sintering, demonstrated different ratios of adhesive, cohesive, and mixed failure modes. A greater number of failures were associated with the combined failure. Table 3 lists the percentile distribution of failure modes.

Scanning Electron Microscopy Evaluation. Scanning electron micrographs of zirconia disks/cement interfaces are shown in Fig 4. The interface observed in untreated (Fig 4a) and treated with Al_2O_3 before sintering (Fig 4d) only revealed the juxtaposition of cement, while few irregularities were noted in samples treated with Al_2O_3 after sintering (Fig 4b), and an interface of soft mechanical imbrication was noted in samples treated with SiO before sintering (Fig 4e). The surface treatment with SiO after sintering suggests interposition of silica (Fig 4c).

Scanning Electron and Confocal Laser Scanning Microscopy Evaluations of Surface Morphology. Scanning electron micrographs showed a smooth surface without extensive grooves at untreated specimens (Fig 5a), and minimal changes in surfaces treated with Al_2O_3 after sintering (Fig 5b). In specimens treated with SiO after sintering (Fig 5c), silica deposits and grooves with a short extension and depth were found. The surface micrograph of specimens treated with Al_2O_3 before sintering (Fig 5d) showed superficial defects with a granular appearance, and the surface changes observed in specimens treated with SiO be-

Table 3 Percentile Distribution of Failure Modes for Different Surface Treatments

| Failure mode	Surface treatment AL	ALS	C	RO	ROS
Adhesive	27	27	28	20	5
	93.10%	90%	100%	76.92%	17.24%
Cohesive	0	0	0	0	1
	0%	0%	0%	0%	3.45%
Mixed	2	3	0	6	23
	6.90%	10%	0%	23.08%	79.31%
Total of observations	29	30	28	26	29

Missing frequency = 8.

fore sintering (Fig 5e) suggest silica deposition and a granular appearance.

The confocal laser micrographs are shown in Fig 6. In analyzing surface morphology, it was noted that untreated (Fig 6a), treated with Al_2O_3 after sintering (Fig 6b), and treated with SiO after sintering (Fig 6c) presented a plain but rough surface and that there was great destruction of the surface and evident irregularities in surfaces treated before sintering with Al_2O_3 (Fig 6d) and SiO (Fig 6e).

The results of surface roughness are presented in Fig 7. The roughness analyses revealed that untreated specimens showed statistical similarity to those treated after sintering, with Al_2O_3 ($P = .12$) and SiO ($P = .08$), while those treated before sintering with
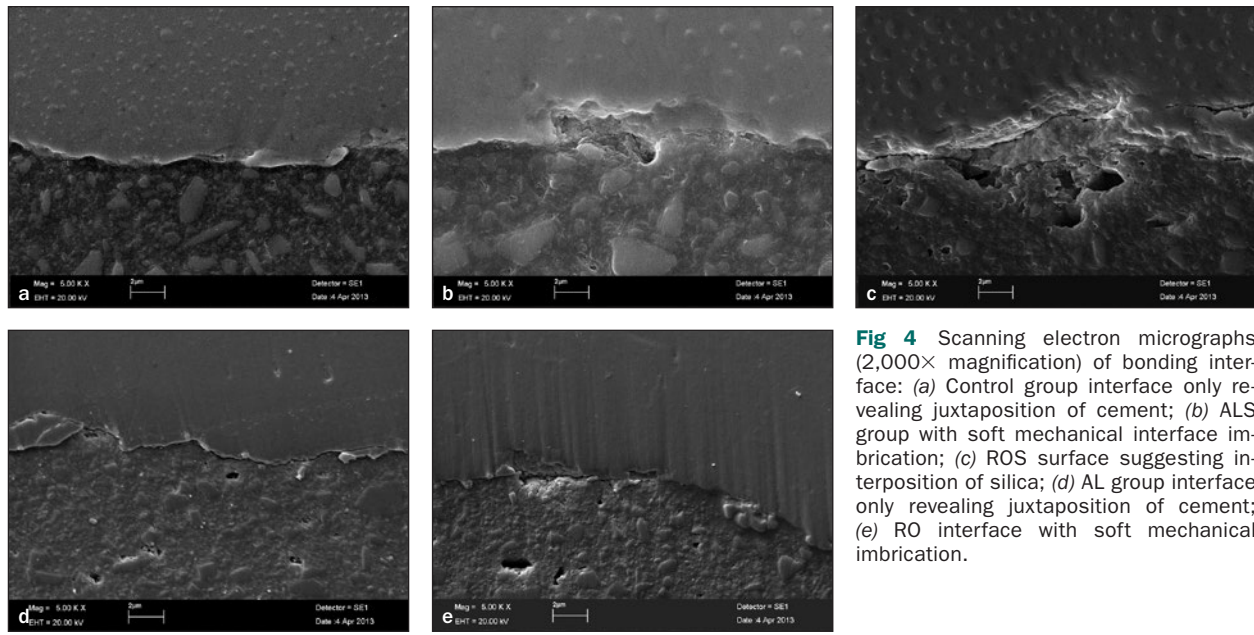
Fig 4 Scanning electron micrographs (2,000× magnification) of bonding interface: *(a)* Control group interface only revealing juxtaposition of cement; *(b)* ALS group with soft mechanical interface imbrication; *(c)* ROS surface suggesting interposition of silica; *(d)* AL group interface only revealing juxtaposition of cement; *(e)* RO interface with soft mechanical imbrication.
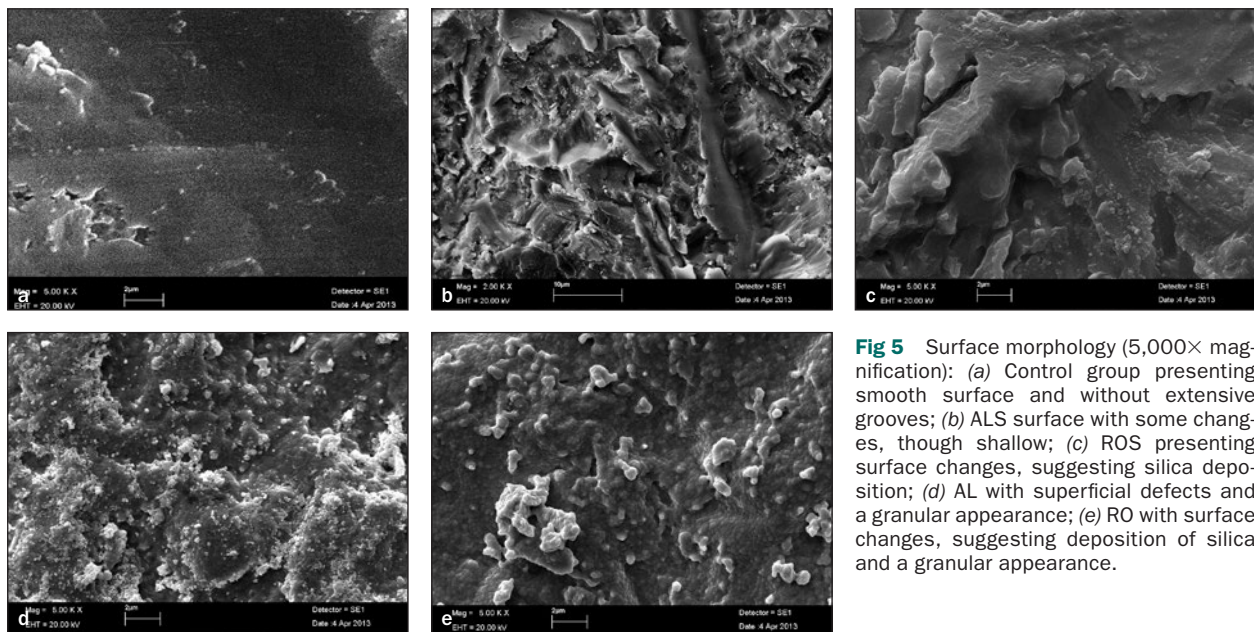
Fig 5 Surface morphology (5,000× magnification): *(a)* Control group presenting smooth surface and without extensive grooves; *(b)* ALS surface with some changes, though shallow; *(c)* ROS presenting surface changes, suggesting silica deposition; *(d)* AL with superficial defects and a granular appearance; *(e)* RO with surface changes, suggesting deposition of silica and a granular appearance.

Al_2O_3 achieved the highest Ra values and statistical difference ($P < .01$) among the other groups (Table 4).

Part 2: Fatigue Resistance and Failure Mode of Zirconia Crowns Bonded to Zirconia Abutments

Misfit Analysis. Figure 8 shows misfit values of copings on the abutments. The group treated with SiO before sintering had the highest misfit values. Smaller misfit values were presented by the untreated group, which in turn was similar to groups treated after sintering with Al_2O_3 ($P = .15$) and SiO ($P = .23$) (Table 5).

Confocal laser scanning images of marginal misfits are shown in Fig 9. Similar spaces are presented by groups: untreated (Fig 9a), treated after sintering with Al_2O_3 (Fig 9b) and SiO (Fig 9c), and more pronounced irregularities by groups treated before sintering with Al_2O_3 (Fig 9d) and SiO (Fig 9e), which corroborates with the misfit values found (Table 5).

Fatigue Test. The fatigue resistance and survival rates of the analog-abutment-crown assemblies are shown in Tables 6 and 7. For the untreated group, samples failed at a mean load of 277.1 N, and one specimen withstood all 140,000 cycles (survival 3.9%
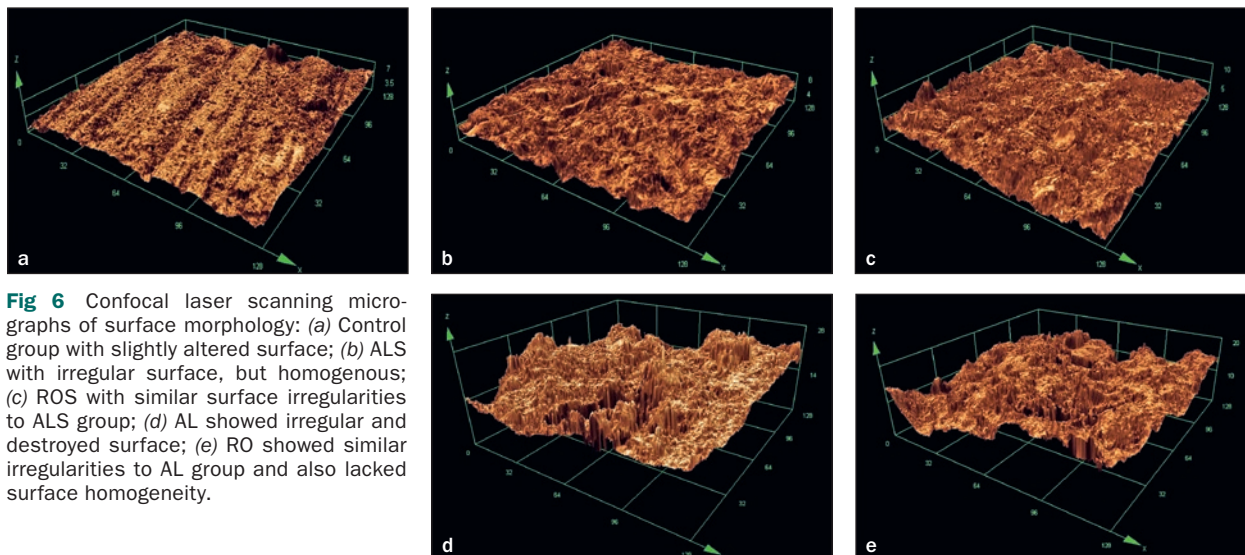
Fig 6 Confocal laser scanning micrographs of surface morphology: *(a)* Control group with slightly altered surface; *(b)* ALS with irregular surface, but homogenous; *(c)* ROS with similar surface irregularities to ALS group; *(d)* AL showed irregular and destroyed surface; *(e)* RO showed similar irregularities to AL group and also lacked surface homogeneity.

Fig 7 Surface roughness results.
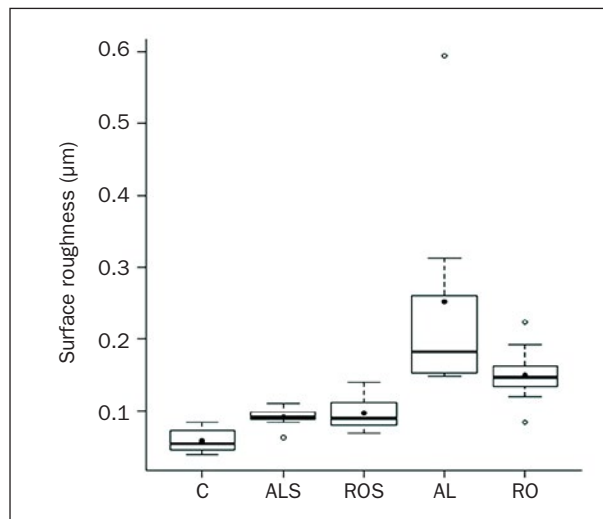
Table 4   Surface Roughness Comparison Among Different Surface Treatments

|	Variable required log transformation				Geometric mean			
	Mean difference	P value	Confidence interval[a]			Mean difference	Confidence interval[a]		
Comparison			Lower limit	Upper limit			Lower limit	Upper limit
AL × ALS	0.88	< .01	0.33	1.43		0.127	0.046	0.218
AL × C	1.35	< .01	0.80	1.90		0.162	0.091	0.244
AL × RO	0.40	.25	−0.15	0.95		0.072	−0.027	0.176
AL × ROS	0.84	< .01	0.29	1.39		0.124	0.041	0.216
ALS × C	0.47	.12	−0.08	1.02		0.034	−0.005	0.077
ALS × RO	−0.48	.12	−1.03	0.07		−0.055	−0.123	0.009
ALS × ROS	−0.04	.99	−0.59	0.51		−0.004	−0.055	0.048
C × RO	−0.95	< .01	−1.50	−0.40		−0.090	−0.149	−0.037
C × ROS	−0.51	.08	−1.06	0.04		−0.038	−0.081	0.003
RO × ROS	0.44	.18	−0.11	0.99		0.052	−0.013	0.121

[a]Adjustment by Tukey.
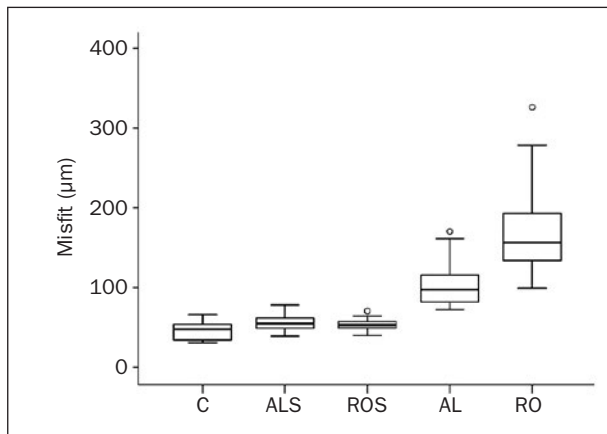
Fig 8 Misfit results measured by confocal laser scanning microscopy.

Table 5	Marginal Misfit (µm) Among Tested Groups
Group	Mean (95% CI)
C	46.21 (42.62–49.79)[a]
AL	104.7 (95.24–114.16)[b]
ALS	55.08 (51.83–58.32)[a]
RO	171.53 (155–188.07)[c]
ROS	53.05 (50.17–55.92)[a]

*Groups identified with different letters show significant differences (ANOVA and Tukey test, $P < .01$).
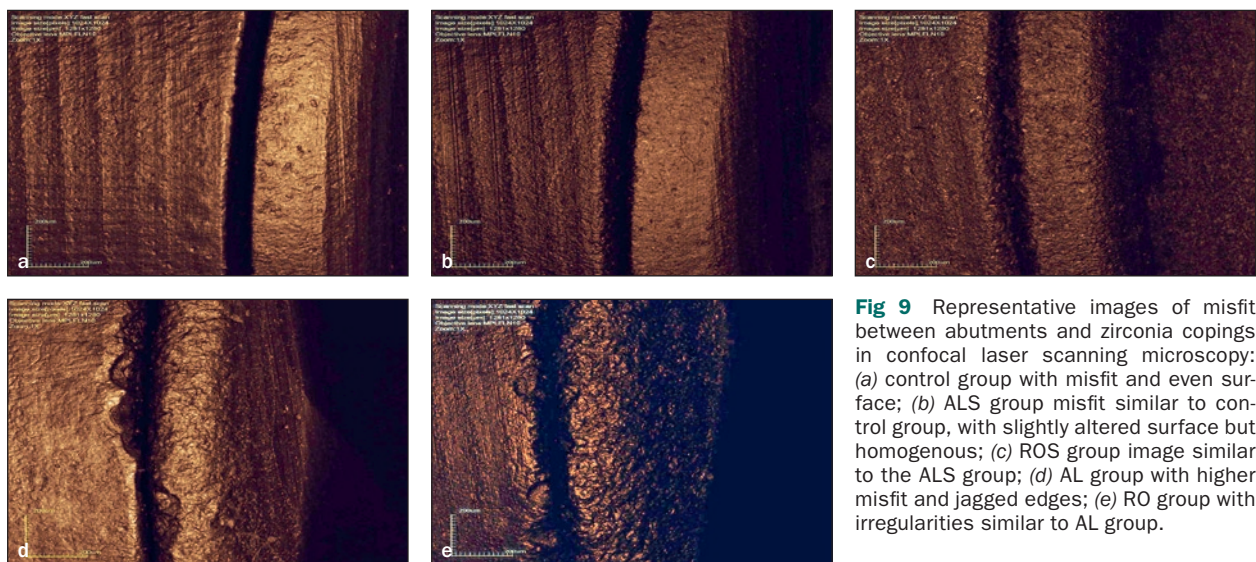
Fig 9 Representative images of misfit between abutments and zirconia copings in confocal laser scanning microscopy: (a) control group with misfit and even surface; (b) ALS group misfit similar to control group, with slightly altered surface but homogenous; (c) ROS group image similar to the ALS group; (d) AL group with higher misfit and jagged edges; (e) RO group with irregularities similar to AL group.

without damage); for the group treated before sintering with Al_2O_3, the mean fracture load was 289.2 N, and three specimens survived the test (13.9% survival); the group treated after sintering with Al_2O_3 found a mean load of 271.4 N with two samples intact after the test (survival 8.6%); for the group treated before sintering with SiO, the samples failed at a mean load of 270.7 N, and no specimens withstood all 140,000 cycles; lastly, the group treated after sintering with SiO had a mean load of 268.5 N, and two samples survived to the end of all cycles (9.5% survival). No significant difference was found for survival rates between the groups tested ($P = .57$) (Fig 10). All experimental groups presented similar failure modes (Table 7), with a higher number of abutment failures (type I), except for the untreated group, which showed a higher number of veneer failures (type II). There was no exclusively coping failure (type III). Images of flaws found in macroscopic patterns are shown in Fig 11. Checking the correlation between marginal misfit values and number of cycles/load stage through the Spearman correlation coefficient that ranges from –1 to 1, it was determined that there was no significant correlation (Table 8).

DISCUSSION

The present study proposed different surface treatments at the zirconia surface in order to improve the bond strength of resin cement to zirconia; nevertheless, the effects of these surface treatments were not only evaluated by micro shear bond strength tests, but zirconia abutments and crowns were submitted to fatigue tests after submitting to the same treatments. Then, it was possible to know if the better micro shear bond strength interferes with the clinical behavior (survival probability) of these abutments and crowns. The null hypothesis was partially rejected because the

Table 6 Survival Probability (%) Per Load Stage

Groups	Load (N)	No. of samples starting the cycle	No. of samples that failed	Survival probability (%) (95% CI)
C	80	14	–	100
	120	14	–	100
	160	14	1	92.9 (59.1–99)
	200	13	2	78.6 (47.3–92.5)
	240	11	1	71.4 (40.6–88.2)
	280	10	3	50.0 (22.9–72.2)
	320	7	6	3.9 (0.1–24.3)
AL	80	13	–	100
	120	13	–	100
	160	13	1	92.3 (46.6–98.9)
	200	12	1	84.6 (51.2–95.9)
	240	11	1	76.9 (44.2–91.9)
	280	10	1	69.2 (37.3–87.2)
	320	9	6	13.9 (1.5–39.2)
ALS	80	14	–	100
	120	14	–	100
	160	14	–	100
	200	14	2	85.7 (53.9–96.2)
	240	12	5	50.0 (22.9–72.2)
	280	7	1	42.9 (17.7–66)
	320	6	4	8.6 (0.5–31.5)
RO	80	13	–	100
	120	13	–	100
	160	13	1	92.3 (56.6–98.9)
	200	12	2	76.9 (44.2–91.9)
	240	10	3	53.9 (24.8–76)
	280	10	3	53.9 (24.8–76)
	320	7	7	–
ROS	80	14	–	100
	120	14	–	100
	160	14	1	92.9 (59.1–99)
	200	13	1	85.7 (53.9–96.2)
	240	12	3	64.3 (34.3–83.3)
	280	9	5	28.6 (8.8–52.4)
	320	4	2	9.5 (0.6–33.5)

Table 7 Failure Mode Distribution (%) Among the Tested Groups

Failure mode	Groups (%)				
	AL	ALS	C	RO	ROS
I	31	43	21.4	76.9	50
II	23	14.2	42.8	15.3	21.4
III	0	0	0	0	0
IV	0	0	14.2	0	0
V	23	28.5	14.2	7.6	14.2

Type I = Abutment failure; type II = veneers failure; type III = coping failure; type IV = abutment and coping failure; type V = abutment and veneer failure.

Table 8 Cycles/Load Stage: Spearman Correlation Coefficient

Groups	Spearman coefficient (load × misfit)	Spearman coefficient (cycles × misfit)
C	−0.325	−0.169
AL	−0.040	−0.104
ALS	−0.371	−0.377
RO	−0.156	−0.033
ROS	0.374	0.330
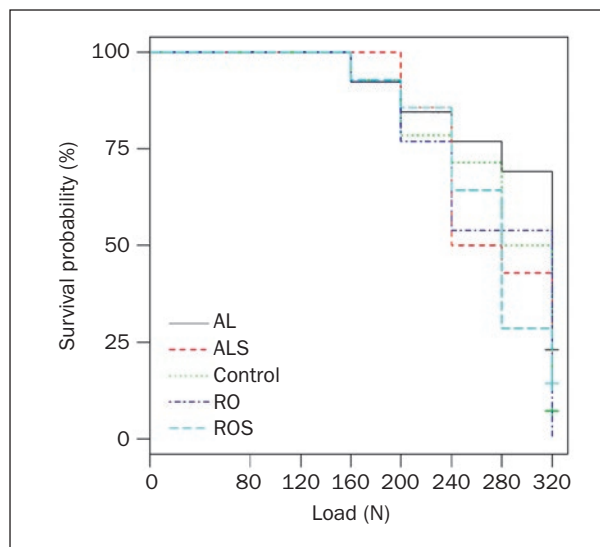
Fig 10 Survival probability among groups tested (life table survival analysis).
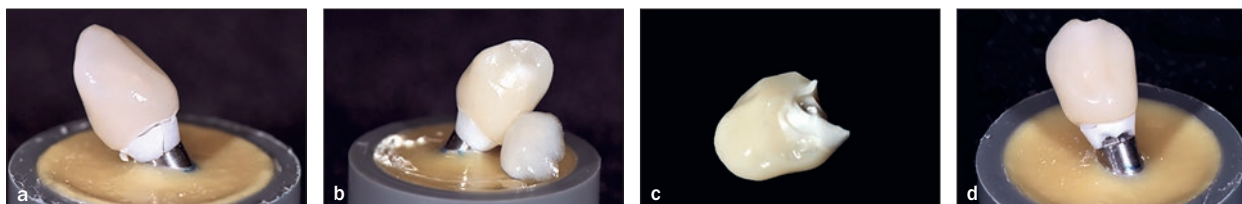
Fig 11 Failure mode photographs: *(a)* Type I (abutment); *(b)* Type II (veneer); *(c)* Type IV (abutment and coping); *(d)* Type V (abutment and veneer).

micro shear bond strength of zirconia to resin cement was affected by the surface treatment; however, the same surface treatments did not influence the fatigue resistance and failure mode of crowns bonded to zirconia abutments, showing that better micro shear bond strength of a surface treatment does not affect mechanical behavior of abutments and crowns submitted to the same surface treatment.

Surface treatment before sintering was proposed because there is no consensus about the effect of airborne particle abrasion after sintering.[15–17] Some authors believed that air abrasion could introduce defects and weaken the zirconia surface; others argued that tetragonal-monoclinic transformation caused by air abrasion causes a volume increase with compressive stress that heals these defects.

Part 1: Micro Shear Bond Strength of Resin-Based Cement to Zirconia

Silicatization of zirconia resulted in higher micro shear bond strength compared with the control. This probably occurred due to the silica-coating system, which applies two sandblasting procedures to the surface before the application of a resin, which may create a larger active surface by first sandblasting the surface with Al_2O_3 and then forming a silica layer by blasting the surface with special silica particles. The silane applied likely enhances the bond between the silica within the ceramic surface and the organic groups of the applied luting resin, since the silica layer has been shown to be well attached to the ceramic surface.[18] Similar results were observed by other authors[19] who demonstrated a similar effect for the silica-coating system on the shear bond strength of densely sintered high-purity aluminum oxide specimens, indicating that silica coating was an efficient way of increasing the shear bond strength of the ceramic.

On the other hand, the groups treated with Al_2O_3 were similar to the control, which is in agreement with the findings of several studies[1,19,20] that reported bond strengths to zirconia ceramics that did not improve after airborne-particle abrasion. Some authors[1,20] reported that certain roughness is produced by airborne particle abrasion, but there are limited undercuts that are insufficient to improve bonding to zirconia.

Zirconia bond strength may be improved by airborne-particle abrasion and silica coating of yttria-stabilized zirconia surfaces before sintering without damaging the microstructure,[10] but few studies have assessed this alternative conditioning method. In the present study, the surface treatment with silica before or after sintering influenced the adhesion, but the same does not happen for aluminum oxide treatment. The group that was treated with Al_2O_3 before sintering was similar to the untreated group and the group that was treated with Al_2O_3 after sintering, while the group that was treated with SiO before sintering achieved higher bond strength values than the untreated group but was statistically lower than that treated with SiO after sintering. A previous study[10] corroborated the results for both groups treated with Al_2O_3 in the present study; the groups treated with Al_2O_3 before and after sintering following the same parameters of airborne particle abrasion were statistically similar. On the other hand, the present study found higher bond strength values for the group treated with SiO after sintering than that treated before sintering, and for these than untreated while tribochemical silica coating before sintering was shown to be inefficient, with similar results to nonconditioned zirconia in a previous study.[10] This difference is probably attributed to the particle size difference, which was greater in the present study (110 µm SiO) than in the previous study (30 µm SiO), and the parameters used for air abrasion in the previous study used greater pressure (2 bars) and time (15 seconds) and lower distance (10 mm).

It seems that the sintering process of zirconia may lead to the loss of silica coating; thus, the zirconia surface loses the ability to form chemical bonds and presents similar micro shear bond strength values to the air abrasion groups. The failure mode on almost all of the specimens in the group treated with SiO after sintering was mixed failure. In both groups treated with Al_2O_3 and the group treated with SiO before sintering, mixed failures occurred, but there was a predominance of adhesive failures in more than 50% of the specimens (Table 3). This failure mode difference might have been caused by the highly irregular silica surface, resulting in an improved contact area between the zirconia surface and resin cement. Another reason for the mixed failures of the group treated with SiO after sintering is that according to the manufacturer, RelyX U200 contains methacrylate monomers, adhesive phosphate monomer, and silanated fillers in its chemical composition, and bonding to zirconia is improved after silica coating and silane application because of adhesive phosphate monomer,[21] which sometimes exceeds its own cohesive strength. For the untreated group, the failure mode was only adhesive, while for both groups treated with Al_2O_3 and the group treated with SiO before sintering, mixed failures occurred, but there was also a predominance of adhesive failures. The predominance of adhesive failures for these groups can be explained by the zirconia characteristics in each surface treatment, considering that limited undercuts were produced after sandblasting, thus not improving bonding to zirconia.

In the present study, confocal laser and scanning electron microscopy analyses were used to observe topography changes after different surface treatments

and to analyze surface roughness. In scanning electron images, the control group showed a relatively smooth surface without extensive grooves (Fig 5a) and an interface with cement juxtaposition (Fig 4a), which might explain the findings related to the micro shear bond strength data and failure mode analysis. Similar results were found for the group treated after sintering with Al_2O_3, where some surface changes occurred, although they were shallow (Figs 4b and 5b). In the group treated with SiO after sintering, scanning electron micrographs indicated surface modifications suggesting silica deposition and justifying the high micro shear bond strength values (Figs 4c and 5c). On the other hand, the groups treated before sintering with Al_2O_3 (Figs 4d and 5d) and SiO (Figs 4e and 5e) showed surface modifications with a granular aspect, although in the images for the last suggested silica deposition, the micro shear bond strength was lower, likely due to the pattern of surface modification.

The confocal laser scanning microscopy observation corroborates with the findings of the scanning electron microscopy evaluation. Moreover, these images (including the roughness analyses) confirm that although there is greater surface irregularity on disks treated before sintering (Figs 6d and 6e), these irregularities that could contribute to increased mechanical retention are not homogenous and therefore are not able to increase the micro shear bond strength. Homogenous surfaces were produced in the groups that received airborne particle abrasion after sintering (Figs 6b and 6c), which contributed to higher micro shear bond strength values, although the roughness values were lower. Also, the group treated after sintering with SiO obtained the highest micro shear bond strength values, indicating that silica coating promoted chemical bonding at the ceramic-resin cement interface, but did not result in frank surface modifications (Fig 6c). Future studies are necessary to evaluate the effect of different particle sizes and application time on the surface of zirconia without accelerating the formation of surface micro-cracks that could compromise the quality of the substrate.[1]

Part 2: Fatigue Resistance and Failure Mode of Zirconia Crowns Bonded to Zirconia Abutments

The surface treatments performed before cementation increased marginal gaps. In this analysis, both groups treated before sintering had the highest misfit values. The untreated group presented smaller mismatch values, which in turn were similar to the groups treated after sintering (Table 5). Thus, since nonsintered copings (RO and AL groups) have more sensitive surfaces to blasting, even though it is a different blasting protocol, the thinner structure at the coping edge makes

them more susceptible to loss of structure, and consequently, there is an increased marginal gap that can be observed in the confocal laser micrographs (Figs 9d and 9e). Some authors[22] have suggested that the surface treatment before cementation can lead to an increase of marginal gaps since airborne particle abrasion, which is a required step of the silicatization method before cementation, has been reported to cause marginal defects, increasing the space between the crown and the abutment. On the other hand, the groups treated with Al_2O_3 and SiO that were already sintered prior to treatments showed misfit values similar to the control group. Additionally, it is important to consider that surface roughness is affected differently by surface treatments, and surface treatments performed before sintering lead to greater surface roughness, possibly interfering with crown seating and greater marginal misfit.

In this study, copings were not cemented before the evaluation, as when samples are cemented, they may lose the accuracy of the primary adjustment, thereby allowing the influence of cement type, viscosity, and cementation techniques.[23] The accuracy of marginal fit was assessed by confocal laser scanning microscopy direct visualization and external measurements (Table 5). Direct visualization has the advantage of being nondestructive and therefore is applicable to clinical practice, simplifying sample preparation and making the method viable and reproducible. According to the literature, average misfit in the range of 100 to 120 μm is considered clinically acceptable.[24] In this regard, both groups treated before sintering presented greater misfit, especially the group treated with SiO, whose marginal misfit (171.53 μm) is greater than clinically acceptable values. Considering higher misfit values of samples treated before sintering, the careful use of air abrasion techniques before sintering is advisable to minimize marginal defects.

The experimental protocol of this study is a modification of norm ISO 14801. An isometric loading protocol was used for the mechanical fatigue test with 5 Hz frequency at 80 N, followed by stages of 120, 160, 200, 240, 280, and 320 N, with a maximum of 20,000 cycles in each stage. This loading protocol was used in several studies[13,14,25,26] because it covers a wide range of clinically relevant situations. Some authors[13,27] revealed that the benefit of this type of test is that it provides better simulation of clinical conditions than a static load test and does not require an extensive period of testing. In vitro studies[28–30] investigating zirconia abutments demonstrated that high loads are required to fracture specimens. The first part of the test is within the range of realistic occlusion forces in the anterior region, eg, up to 100 N.[25] The second part comprises a load range that can be found in bruxism, trauma

(extrinsic high loads), or masticatory intrinsic accidents (under chewing load, but concentrated in a small area due to a hard foreign body such as a stone or seed, for example). Also, a flat composite resin surface was used as an antagonist as suggested in other similar fatigue studies[13,14,31] in order to prevent localized and intense point loads and unrealistic surface damage.[32] Flexibility and antagonist wear allowed the most realistic simulation of tooth contact through a wear facet included in the incisal edge of the restoration. The large and uniform contact surface prevented intense load points, which could exceed the restorative materials compressive limits and produce surface damage and debris powder by crushing.

With mean fracture loads between 268 and 289 N (group treated with SiO after sintering and group treated with Al_2O_3 before sintering, respectively) and acceptable survival rates within the real occlusal strength, it seems that all experimental groups presented adequate performance. The critical loads for metallic and ceramic implant abutments restored with ceramic crowns have been assessed by some studies with results ranging between 170 and 1,454 N.[33–35] Some authors[36] showed a mean load of 340 N for fracture resistance of zirconia abutments associated with crowns, which differs from the values found in this study. However, the methodology employed static loads, which overestimate the fracture resistance values, not revealing the reality used in the fatigue tests.

The lack of difference in the survival probability among the groups tested reveals that the proposed surface treatments did not influence their mechanical properties, which makes their use feasible in this aspect. Thus, the hypothesis that the treatments would not influence the mechanical behavior of the analog-abutment-crown sets was accepted. The failure modes were mostly type I exclusively on the abutment; only the control group showed predominance of failure exclusively in the veneer (Type II). The abutment failure mode analysis revealed that the fracture is common in the cervical portion close to the implant interface. Thus, the failure mode of ceramic abutments in this study is comparable to the findings of other in vitro studies.[34] The cervical region of abutments is the area of greatest stress concentration generated due to tooth positioning during the load application; therefore, the abutment-analog interface is the weakest point in the set.[22,31] The findings of a previous study[37] confirm the results of this study, pointing to similar failure modes after a fracture resistance test of zirconia abutments associated with external hex implants. According to another analysis,[38,39] a comparison of titanium and zirconia abutments revealed that when titanium abutments are used, no failures occur in the abutments, but the screws often fracture, showing that in this system, the weakest link is the screw because there is greater tension concentration and torque. Moreover, the same load caused zirconia abutment fracture, but the screws were intact, as occurred in this study, and this can be explained by the low tolerance of zirconia for tensile forces. With that point of view, this can be considered an advantage of zirconia abutments, as a fractured abutment can be easily replaced. However, with a fractured screw, removal and replacement becomes even more complex.

The analysis of the correlation between marginal gap values and number of cycles/load stage through the Spearman correlation coefficient determined that there was no significant correlation. These results agree with other authors[40] who did not find correlation between misfit and fracture strength in internal Morse type connection.

The similar survival probability of samples submitted to different surface treatments suggests that mechanical behavior of abutments and crowns was not affected by surface treatments after sintering. Air abrasion after sintering probably avoids surface defects of zirconia through tetragonal-monoclinic transformation and healing of defects, but future studies evaluating yttria-stabilized zirconia phases are necessary to confirm this hypothesis.

CONCLUSIONS

Within the limitations of this study, it was possible to conclude that micro shear bond strength is improved after silica-coating surface treatment after sintering, but mechanical behavior of crowns/abutments/implants was not affected by different surface treatments.

ACKNOWLEDGMENTS

REFERENCES

1. de Oyagüe RC, Monticelli F, Toledano M, Osorio E, Ferrari M, Osorio R. Influence of surface treatments and resin cement selection on bonding to densely-sintered zirconium-oxide ceramic. Dent Mater 2009;25:172–179.

2. Jevnikar P, Krnel K, Kocjan A, Funduk N, Kosmac T. The effect of nano-structured alumina coating on resin-bond strength to zirconia ceramics. Dent Mater 2010;26:688–696.

3. Amaral R, Ozcan M, Bottino MA, Valandro LF. Microtensile bond strength of a resin cement to glass infiltrated zirconia-reinforced ceramic: The effect of surface conditioning. Dent Mater 2006;22:283–290.

4. Atsu SS, Kilicarslan MA, Kucukesmen HC, Aka PS. Effect of zirconium-oxide ceramic surface treatments on the bond strength to adhesive resin. J Prosthet Dent 2006;95:430–436.

5. Kumbuloglu O, Lassila LV, User A, Vallittu PK. Bonding of resin composite luting cements to zirconium oxide by two air-particle abrasion methods. Oper Dent 2006;31:248–255.

6. Wolfart M, Lehmann F, Wolfart S, Kern M. Durability of the resin bond strength to zirconia ceramic after using different surface conditioning methods. Dent Mater 2007;23:45–50.

7. Bottino MA, Valandro LF, Scotti R, Buso L. Effect of surface treatments on the resin bond to zirconium-based ceramic. Int J Prosthodont 2005;18:60–65.

8. Ozcan M, Alkumru HN, Gemalmaz D. The effect of surface treatment on the shear bond strength of luting cement to a glass-infiltrated alumina ceramic. Int J Prosthodont 2001;14:335–339.

9. Zhang Y, Lawn BR, Rekow ED, Thompson VP. Effect of sandblasting on the long-term performance of dental ceramics. J Biomed Mater Res B Appl Biomater 2004;71:381–386.

10. Monaco C, Cardelli P, Scotti R, Valandro LF. Pilot evaluation of four experimental conditioning treatments to improve the bond strength between resin cement and Y-TZP ceramic. J Prosthodont 2011;20:97–100.

11. Karimipous-Saryazdi M, Sadid-Zadeh R, Givan D, Burgess JO, Ramp LC, Liu PR. Influence of surface treatment of yttrium-stabilized tetragonal zirconium oxides and cement type on crown retention after artificial aging. J Prosthet Dent 2014;111:395–403.

12. Naves LZ, Santana FR, Castro CG, et al. Surface treatment of glass fiber and carbon fiber posts: SEM characterization. Microsc Res Tech 2011;74:1088–1092.

13. Magne P, Knezevic A. Simulated fatigue resistance of composite resin versus porcelain CAD/CAM overlay restorations on endodontically treated molars. Quintessence Int 2009;40:125–133.

14. Magne P, Paranhos MP, Burnett LH Jr. New zirconia primer improves bond strength of resin-based cements. Dent Mater 2010;26:345–352.

15. Aurélio IL, Marchionatti AME, Montagner AF, May LG, Soares FZM. Does air particle abrasion affect the flexural strength and phase transformation of Y-TZP? A systematic review and meta-analysis. Dent Mater 2016;32:827–845.

16. Ramos-Tonello CM, Trevizo BF, Rodrigues RF, et al. Pre-sintered Y-TZP sandblasting: Effect on surface roughness, phase transformation, and Y-TZP/veneer bond strength. J Appl Oral Sci 2017;25:666–673.

17. Okada M, Taketa H, Torii Y, Irie M, Matsumoto T. Optimal sandblasting conditions for conventional-type yttria-stabilized tetragonal zircônia polycristals. Dent Mater 2019;35:169–175.

18. Kern M, Thompson VP. Sandblasting and silica coating of a glass-infiltrated alumina ceramic: Volume loss, morphology, and changes in the surface composition. J Prosthet Dent 1994;71:453–461.

19. Blixt M, Adamczak E, Lindén LA, Odén A, Arvidson K. Bonding to densely sintered alumina surfaces: Effect of sandblasting and silica coating on shear bond strength of luting cements. Int J Prosthodont 2000;13:221–226.

20. Casucci A, Monticelli F, Goracci C, et al. Effect of surface pre-treatments on the zirconia ceramic-resin cement microtensile bond strength. Dent Mater 2011;27:1024–1030.

21. Nothdurft FP, Motter PJ, Pospiech PR. Effect of surface treatment on the initial bond strength of different luting cements to zirconium oxide ceramic. Clin Oral Investig 2009;13:229–235.

22. Att W, Hoischen T, Gerds T, Strub JR. Marginal adaptation of all-ceramic crowns on implant abutments. Clin Implant Dent Relat Res 2008;10:218–225.

23. Hamza TA, Ezzat HA, El-Hossary MM, Katamish HA, Shokry TE, Rosenstiel SF. Accuracy of ceramic restorations made with two CAD/CAM systems. J Prosthet Dent 2013;109:83–87.

24. Beuer F, Naumann M, Gernet W, Sorensen JA. Precision of fit: Zirconia three-unit fixed dental prostheses. Clin Oral Investig 2009;13:343–349.

25. Ferrario VF, Sforza C, Serrao G, Dellavia C, Tartaglia GM. Single tooth bite forces in healthy young adults. J Oral Rehabil 2004;31:18–22.

26. Kuijs RH, Fennis WM, Kreulen CM, Roeters FJ, Verdonschot N, Creugers NH. A comparison of fatigue resistance of three materials for cusp-replacing adhesive restorations. J Dent 2006;34:19–25.

27. Fennis WM, Kuijs RH, Kreulen CM, Verdonschot N, Creugers NH. Fatigue resistance of teeth restored with cuspal-coverage composite restorations. Int J Prosthodont 2004;17:313–317.

28. Aramouni P, Zebouni E, Tashkandi E, Dib S, Salameh Z, Almas K. Fracture resistance and failure location of zirconium and metallic implant abutments. J Contemp Dent Pract 2008;9:41–48.

29. Kerstein RB, Radke J. A comparison of fabrication precision and mechanical reliability of 2 zirconia implant abutments. Int J Oral Maxillofac Implants 2008;23:1029–1036.

30. Adatia ND, Bayne SC, Cooper LF, Thompson JY. Fracture resistance of yttria-stabilized zirconia dental implant abutments. J Prosthodont 2009;18:17–22.

31. Magne P, Paranhos MP, Burnett LH Jr, Magne M, Belser UC. Fatigue resistance and failure mode of novel-design anterior single-tooth implant restorations: Influence of material selection for type III veneers bonded to zirconia abutments. Clin Oral Implants Res 2011;22:195–200.

32. Kelly JR. Clinically relevant approach to failure testing of all-ceramic restorations. J Prosthet Dent 1999;81:652–661.

33. Cho HW, Dong JK, Jin TH, Oh SC, Lee HH, Lee JW. A study on the fracture strength of implant-supported restorations using milled ceramic abutments and all-ceramic crowns. Int J Prosthodont 2002;15:9–13.

34. Yildirim M, Fischer H, Marx R, Edelhoff D. In vivo fracture resistance of implant-supported all-ceramic restorations. J Prosthet Dent 2003;90:325–331.

35. Sailer I, Sailer T, Stawarczyk B, Jung RE, Hämmerle CH. In vitro study of the influence of the type of connection on the fracture load of zirconia abutments with internal and external implant-abutment connections. Int J Oral Maxillofac Implants 2009;24:850–858.

36. Martínez-Rus F, Ferreiroa A, Özcan M, Bartolomé JF, Pradíes G. Fracture resistance of crowns cemented on titanium and zirconia implant abutments: A comparison of monolithic versus manually veneered all-ceramic systems. Int J Oral Maxillofac Implants 2012;27:1448–1455.

37. Truninger TC, Stawarczyk B, Leutert CR, Sailer TR, Hämmerle CH, Sailer I. Bending moments of zirconia and titanium abutments with internal and external implant-abutment connections after aging and chewing simulation. Clin Oral Implants Res 2012;23:12–18.

38. Firidinoğlu K, Toksavul S, Toman M, Sarikanat M, Nergiz I. Fracture resistance and analysis of stress distribution of implant-supported single zirconium ceramic coping combination with abutments made of different materials. J Appl Biomech 2012;28:394–399.

39. Alqahtani F, Flinton R. Postfatigue fracture resistance of modified prefabricated zirconia implant abutments. J Prosthet Dent 2014;112:299–305.

40. Sui X, Wei H, Wang D, et al. Experimental research on the relationship between fit accuracy and fracture resistance of zirconia abutments. J Dent 2014;42:1353–1359.